ACS OMEGA

http://pubs.acs.org/journal/acsodf

Article

Model-Free Adaptive Control of Hydrometallurgy Cascade Gold Leaching Process with Input Constraints

Shijian Dong,* Yuzhu Zhang, Xingxing Zhou, Dapeng Niu, and Xuesong Wang

Cite This: *ACS Omega* 2023, 8, 6559−6570

Read Online

ACCESS | Metrics & More | Article Recommendations

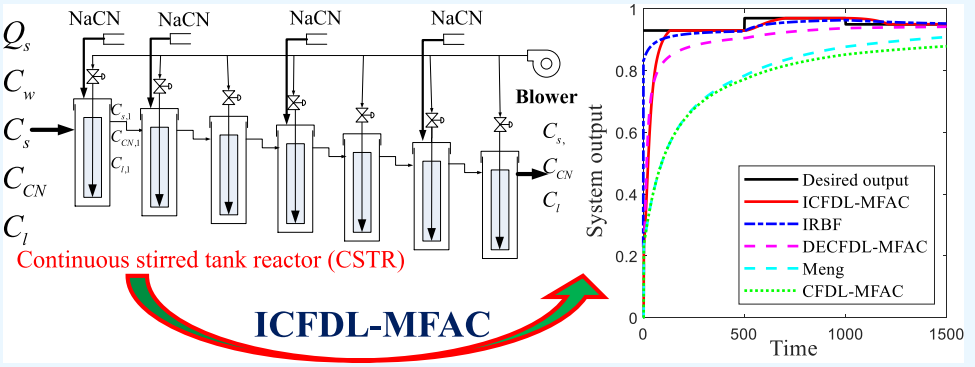

ABSTRACT: Hydrometallurgy technology can directly deal with low grade and complex materials, improve the comprehensive utilization rate of resources, and effectively adapt to the demand of low carbon and cleaner production. A series of cascade continuous stirred tank reactors are usually applied in the gold leaching industrial process. The equations of leaching process mechanism model are mainly composed of gold conservation, cyanide ion conservation, and kinetic reaction rate equations. The derivation of the theoretical model involves many unknown parameters and some ideal assumptions, which leads to difficulty and imprecision in establishing the accurate mechanism model of the leaching process. Imprecise mechanism models limit the application of model-based control algorithms in the leaching process. Due to the constraints and limitations of the input variables in the cascade leaching process, a novel model-free adaptive control algorithm based on compact form dynamic linearization with integration (ICFDL-MFAC) control factor is first constructed. The constraints between input variables is realized by setting the initial value of the input to the pseudo-gradient and the weight of the integral coefficient. The proposed pure data-driven ICFDL-MFAC algorithm has anti-integral saturation ability and can achieve faster control rate and higher control precision. This control strategy can effectively improve the utilization efficiency of sodium cyanide and reduce environmental pollution. The consistent stability of the proposed control algorithm is also analyzed and proved. Compared with the existing model-free control algorithms, the merit and practicability of the control algorithm are verified by the practical leaching industrial process test. The proposed model-free control strategy has advantages of strong adaptive ability, robustness, and practicability. The MFAC algorithm can also be easily applied to control the multi-input multi-output of other industrial processes.

1. INTRODUCTION

Hydrometallurgical technology can effectively extract gold from low-grade gold ore and plays an important role in the field of non-ferrous metal smelting. The hydrometallurgical process can make full use of ore resources and facilitate the recovery of other precious metals.[1−3] Hydrometallurgy is a clean production process, which can satisfy the requirements of environmental protection and low carbon emission. The discipline basis of hydrometallurgy mainly includes physical chemistry of metallurgy, chemical reaction principles, and mechanical engineering.[4] The leaching process is the key process of hydrometallurgy, which determines the extraction efficiency of target products and the difficulty of slag recovery.[5] Gold leaching process is a chemical process in which sodium cyanide solution reacts with gold in the ore. Through the thickening washing process, the cyanide leaching liquid containing sodium gold cyanide can be preliminary separated from the slag.[6] The leaching rate is the key index of the gold leaching process, which determines the quality of the liquid, and it needs to be obtained by the off-line assay.[7] The leaching

Received: October 28, 2022
Accepted: January 30, 2023
Published: February 10, 2023

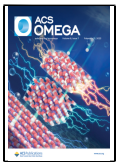

https://doi.org/10.1021/acsomega.2c06830
ACS Omega 2023, 8, 6559−6570

rate directly determines the extraction quality and economic benefit of the subsequent process. The main factors affecting gold cyanidation leaching are cyanide concentration, oxygen concentration, pH value of leaching solution, ore pulp temperature, ore particle size and shape, pulp concentration, leaching time, impurities, and associated minerals.[8] In order to improve the leaching efficiency and reduce the residual amount of sodium cyanide in the leaching process, the addition of sodium cyanide in the cascade leaching process is constrained.[9] The leaching process involves complex multiphase chemical reaction principles and physical knowledge. The complex reaction kinetics mechanism and process random factors increase the difficulty of modeling the cascade leaching process.[10] The working environment of different leaching tanks is not exactly the same. Although the structure of each leaching model is the same, the parameters to be determined are also different.[11] To establish the leaching rate prediction model of the cascade leaching process, it is necessary not only to have complete mechanism knowledge but also to use data mining technology for error compensation.[12] The imprecise model will degrade the performance of the existing model-based control algorithm.[13] Model-free adaptive control techniques do not need to analyze the internal model mechanism and structure of the system.[14] Model-free adaptive control technology can achieve accurate control of complex multivariable systems by adjusting a small number of parameters based on the input and output signals of the system.[15] Model-free adaptive control technology has important advantages for the complex cascade leaching process, which is expected to achieve accurate control and facilitate practical application.

Model-free control technology is a hot topic in scientific theory and engineering application. Researchers have obtained a few scientific research achievements. The proportional-integral-derivative (PID) control algorithm is a typical kind of model-free control method.[16] However, the PID control algorithm needs to use decoupling technology to realize the control of multi-input multi-output (MIMO) system.[17] Another typical model-free adaptive control method is based on neural network adaptive control technology. This kind of control algorithm needs a lot of process data with good performance to train the network.[18] Insufficient training data will lead to poor accuracy and dynamic performance of the controller.[19] For the system with constraints on input and output variables, the control algorithm based on neural networks is difficult to satisfy the control requirements.[20] When the feedback error is less than a certain threshold, the update speed of the neural network control rate will be slow, which leads to a long control time.[21] In contrast, the newly developed model-free adaptive control technology has the advantages of easy engineering implementation and robustness.[22] Based on a simultaneous perturbation approximation, a model-free controller design method has been presented for complex systems with time-varying dynamics, but it cannot control the systems with input constraints.[23] In order to linearize a nonlinear system, a multiple adaptive observer is applied to estimate the pseudo-partial derivative parameter matrix of compact form dynamic linearization. The proposed data-driven method can take control of MIMO nonlinear processes based on the online identified multiobserver models derived from the input/output (I/O) data. The design strategy of this control algorithm can well enlighten the controller design of the leaching process.[24] By using the compact-form-dynamic-linearization-based controller (CFDLc) and partial-form-dynamic-linearization-based controller, a data-driven control method has been presented for discrete-time SISO nonlinear systems. This control algorithm does not rely on the first-principles model and identification model and can control the system well. This result provides a good guide for the engineering application of model-free adaptive control (MFAC) technology.[25] By using a Q-function, the long-term performance of the proposed adaptive controller is estimated. The proposed policy can ensure search of an optimal stabilizing control signal for uncertain and unstable systems. The derived control law does not require an initial stabilizing control assumption. This controller takes into account the common control difficulties of industrial processes such as parametric uncertainty, internal-external nonparametric random uncertainties, and time varying delay.[26] A data-driven MFAC method with dual radial basis function neural networks has been proposed for nonlinear systems. The proposed method provides a systematic design method for controller structure by the direct usage of I/O data. The controller parameters are tuned by the pseudo-gradient (PG) information. This control algorithm does not need to train the system data online, and the applicability of the algorithm is verified in the engineering system.[27] By using constriction coefficient and Hénon chaotic sequences, the model-free learning adaptive control based on PG concepts and optimization procedure by a particle swarm optimization approach has been proposed. The intelligent method used to optimize MFAC control parameters can improve the process control precision, but it will increase the complexity of control parameter adjustment in the leaching process, which is not conducive to industrial application.[28] A different-factor structure-based compact-form model-free adaptive control method with neural networks (DF-CFMFAC-NN) has been proposed for MIMO nonlinear systems. The DF-CFMFAC-NN with learning parameters has powerful tracking ability and flexible design for each control channel. The learning parameters are auto-tuned by back propagation neural networks. This control algorithm has been successfully applied to coal mill system.[29] Combining a sampled-data parameter estimator to estimate the unknown partial derivatives and a sampled-data observer to estimate the residual nonlinear uncertainty, an observer-based SMFAC scheme has been proposed for continuous-time nonlinear nonaffine systems with input constraints. The constraint on the input rate is also considered in the control law as the transition condition. The control algorithm can deal with the constraint input, and it can guide to solve the practical problems of the control input constraint in the leaching process.[30] In order to get the effective tracking trajectory of the lower extremity exoskeleton, a neural network and time-delay estimation technique is added to model-free based iPD controller. The neural network technology can improve the control accuracy of MFAC, but it will increase the difficulty of application in an industrial computer.[31] An adaptive neural network control is designed for the n-link robotic system with full-state constraints. The Moore−Penrose inverse term is employed to prevent the violation of the full-state constraints. The uniform ultimate boundedness of the closed-loop system is guaranteed by using the barrier Lyapunov function. The state constraint technology can provide inspiration for input constraint control technology in the leaching process.[32] A variable structure control in combination with back stepping and Lyapunov synthesis is investigated for MIMO nonlinear

https://doi.org/10.1021/acsomega.2c06830
ACS Omega 2023, 8, 6559−6570

systems with unknown control coefficient matrices and input nonlinearities. Command filters are also presented to implement physical constraints on the virtual control laws. The control technology of the nonlinear system dealing with dead zone input is mainly applied to mechanical systems and is not involved in the leaching process.[33] The neural-network-based output-feedback control strategy is constructed for a class of nonlinear systems. An adaptive dynamic programming algorithm is developed to obtain the desired suboptimal solution with the help of auxiliary quasi-HJB equation. Neural network control technology is a typical model-free control technology, but it is not easy to apply in industrial technology.[34] By simultaneously considering the input saturation and underactuated problems, an adaptive output feedback control for trajectory tracking of underactuated surface vessels. The combination of neural network control technology and MFAC technology is expected to obtain model-free control technology with better performance to promote the development of industry.[35] Based on the simplified mechanism model and the use of intelligent neural network to compensate the unmodeled dynamics in the model, the accurate prediction of the leaching rate in the leaching process has made some progress. It has great significance and application value in the research of leaching process prediction and process operation monitoring. However, the establishment of leaching process model is heavy and not universal. Once the working environment or production conditions change, the model needs to be updated, which limits the implementation of model-based controllers.[36,37] Besides, the model-based control strategy not only has greater computational complexity but also has great engineering application limitations.[38] The MFAC control algorithm based on CFDL has the advantages of simple structure, good algorithm stability, and easy to realize controller design of the actual process. Therefore, this paper will study the MFAC control strategy based on CFDL and design the controller according to the characteristics of the leaching process. Therefore, the model-free adaptive control strategy will be used in this paper to achieve accurate control of the leaching process. These achievements obtained by model-free control strategies provide a good reference and guidance for control of cascade leaching process.

In this paper, a typical cascade leaching process structure is designed and described. The factors affecting the leaching efficiency are introduced and analyzed. The main mechanism model structures and equations involved in the cascade leaching process are also discussed. The complex kinetic reaction mechanism and process random factors may cause the difficulty of accurately modeling the leaching process. A model-free adaptive control strategy with integral regulators is constructed for the first time to control the cascade gold leaching process with input constraints. The stable convergence of the proposed control algorithm is also analyzed. The effectiveness and advantage of the proposed control algorithm will be cross-verified by comparing with the existing methods. The remainder of this paper is organized as below. The hydrometallurgical gold leaching process is introduced and designed in Section 2. The mechanism relationship of the cascade leaching process is given in Section 3. The model-free adaptive control algorithm is proposed in Section 4. The convergence analysis of the MFAC controller is presented in Section 5. The experiment verification is given in Section 6. The results and discussion are given in Section 7. Finally, the main conclusions are drawn in Section 8.

2. HYDROMETALLURGICAL GOLD LEACHING PROCESS

Seven tank reactors in series are adopted to carry out cyanide reaction for the hydrometallurgical gold leaching process as shown in Figure 1. The blower is used to fill each leaching tank

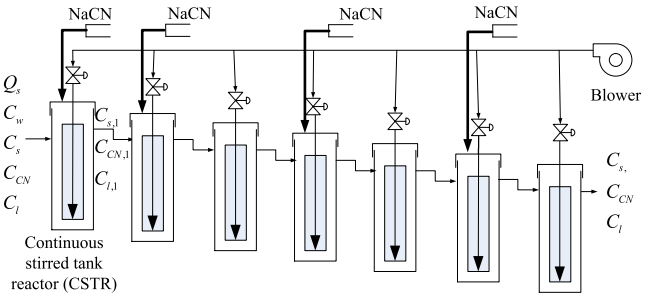

Figure 1. Schematic diagram of the cascade leaching process.

with air. Sodium cyanide is added to the first, second, fourth, and sixth reaction tanks. The ore pulp containing gold is concentrated and stored in buffer tanks. The insoluble gold in the solid phase reacts with sodium cyanide and oxygen to form water-soluble gold cyanide complex ions. Compressed air is passed through the bottom of the leaching tank to provide dissolved oxygen for the reaction. Pneumatic agitation is used to prevent ore pulp accumulation. The reacted ore pulp flows into the subsequent leaching tank through overflow. The cascade leaching process involves complex physical and chemical reactions, and different leaching tanks have different kinetic reaction rates. The leaching process is a complex multiphase chemical reaction process accompanied by the mixing of solid and liquid phases. Leaching reaction involves mechanics, physics, and chemical phenomena. The reaction mechanism of leaching kinetics is very complex and contains random factors. Therefore, there are many factors affecting gold cyanide leaching, mainly as shown in Figure 2.

Ore pulp flow rate, ore pulp concentration, pH value, and dissolved oxygen concentration can be measured online. Gold grade and cyanide ion concentration can only be measured

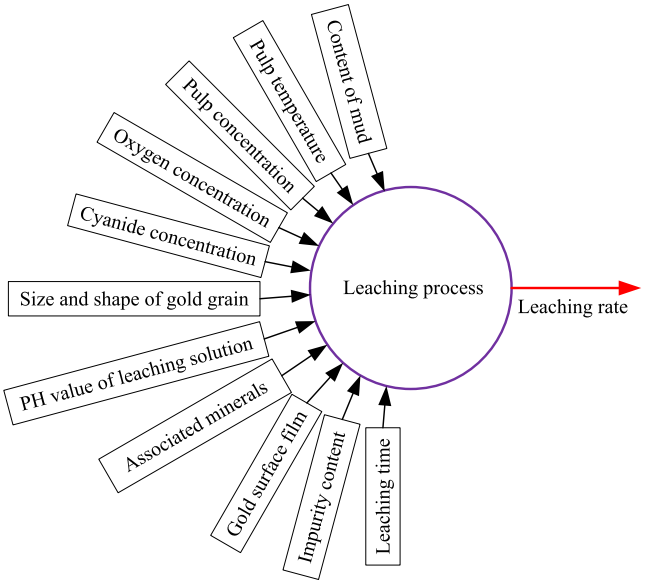

Figure 2. Main influencing factors of the gold leaching process.

https://doi.org/10.1021/acsomega.2c06830
ACS Omega 2023, 8, 6559−6570

offline. Low-frequency and high-frequency disturbances exist in the measurement process, which increase the difficulty of process modeling. The continuous stirred leaching tank reactor also called Pachuca extractor is adopted in the leaching process, as shown in Figure 3. The bottom of the leaching tank

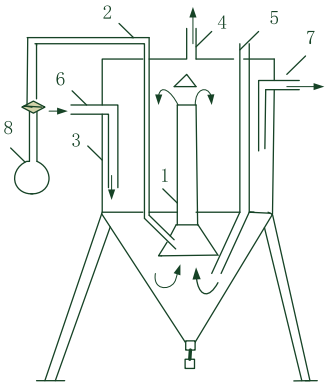

Figure 3. Air-agitation cyanidation leaching tank reactors (Pachuca extractor). (1. Central pipe. 2. Feed pipe. 3. Reaction tank. 4. Exhaust pipe. 5. Auxiliary charging pipe. 6. Ore pulp inlet. 7. Ore pulp discharge. 8. Compressed air pipe).

is filled with compressed air into the central pipe, forming a large number of bubbles rising along the central pipe. The bubble in the central pipe makes the volume of ore pulp expand and the density decrease, which results in the pulp pressure in the central pipe being less than the pressure outside the central pipe. Under the action of pressure difference between the inside and outside of the pipe, the ore pulp in the pipe moves upward and flows out from the upper end of the central pipe. The bubbles that overflow from the ore pulp are discharged through the exhaust pipe at the top of the tank.

The reaction of gold with sodium cyanide is electrochemical dissolution. The oxidation and dissolution of gold occurs at the anode, while the depolarization of oxygen occurs at the cathode, as shown in Figure 4.

The major chemical reactions can be expressed as

$$2Au + 4NaCN + O_2 + 2H_2O \rightarrow 2NaAu(CN)_2 + 2NaOH + H_2O_2 \quad (1)$$

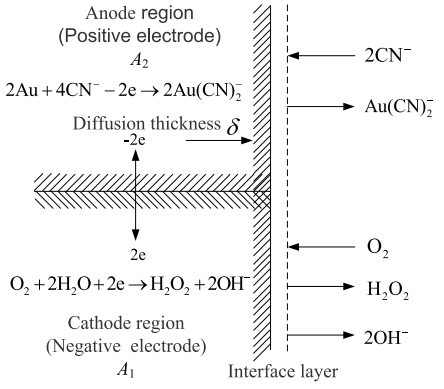

Figure 4. Electrochemical principle of gold cyanidation leaching process. [A_1: Cathode region (negative electrode); A_2: anode region (positive electrode); δ: Nernst interface layer thickness].

The concentration polarization of oxygen and cyanide ion can be determined by Fick's law

$$\frac{d(O_2)}{dt} = \frac{D_{O_2}}{\delta} A_1\{[O_2] - [O_2]_i\} \quad (2)$$

$$\frac{d(CN^-)}{dt} = \frac{D_{CN^-}}{\delta} A_2\{[CN^-] - [CN^-]_i\} \quad (3)$$

where $\frac{d(O_2)}{dt}$ and $\frac{d(CN^-)}{dt}$ are the diffusion rates of O_2 and CN^-, respectively; D_{O_2} and D_{CN^-} are the diffusion coefficients of dissolved oxygen and cyanide ion, respectively; $[O_2]$ and $[CN^-]$ are the concentrations of O_2 and CN^- in the solution, respectively; $[O_2]_i$ and $[CN^-]_i$ are the concentrations of O_2 and CN^- at the interface, respectively.

The chemical reaction rate of O_2 and CN^- at the metal interface is much higher than the diffusion rate, that is, $[O_2]_i \approx 0$, $[CN^-]_i \approx 0$. Eqs 2 and 3 can be simplified as

$$\frac{d(O_2)}{dt} = \frac{D_{O_2}}{\delta} A_1[O_2] \quad (4)$$

$$\frac{d(CN^-)}{dt} = \frac{D_{CN^-}}{\delta} A_2[CN^-] \quad (5)$$

The dissolution rate of gold is twice that of oxygen consumption and half that of cyanide consumption. The dissolution rate of gold v can be expressed as

$$v = \frac{1}{2}\frac{d(CN^-)}{dt} = \frac{1}{2}\frac{D_{CN^-}}{\delta} A_2[CN^-] \quad (6)$$

or

$$v = 2\frac{d(O_2)}{dt} = 2\frac{D_{O_2}}{\delta} A_1[O_2] \quad (7)$$

When the above equation reaches equilibrium

$$\frac{1}{2}\frac{D_{CN^-}}{\delta} A_2[CN^-] = 2\frac{D_{O_2}}{\delta} A_1[O_2] \quad (8)$$

The total surface area of the metal in contact with water can be expressed as $A = A_1 + A_2$. The dissolution rate of gold can be expressed as

$$v = \frac{2AD_{CN^-}D_{O_2}[CN^-][O_2]}{\delta\{D_{CN^-}[CN^-] + 4D_{O_2}[O_2]\}} \quad (9)$$

Since oxygen is cheap and readily available, cyanide is used to control the leaching process rather than oxygen in the control process. The chemical reaction of the leaching process involves many variables and intermediate variables which cannot be directly measured. Therefore, it is very difficult to establish the reaction mechanism model of the leaching process.

3. MECHANISM OF CASCADE LEACHING PROCESS

Existing mechanisms of modeling strategies for leaching processes require the following assumptions. (1) The flow field in the leaching tank is uniformly distributed; (2) the temperature in the leaching tank is uniformly distributed; (3) the slurry stirring in the leaching tank is uniform; (4) mud capacity and resistance are constant; (5) the reaction process is not exothermic; (6) there is no material isolation in the reactor; (7) the oxygen in the pulp can fully react; (8) the

https://doi.org/10.1021/acsomega.2c06830
ACS Omega 2023, 8, 6559−6570

average particle size of the ore is the same; (9) the pH value of the slurry in the leaching tank is constant.

The mechanism model of the leaching process mainly consists of the mass conservation equations of gold in the ore, gold in the liquid, and cyanide ion in the liquid, as well as the corresponding kinetic reaction rate models of gold and cyanide ions. The conservation equation of gold and cyanide in the single tank leaching process can be expressed as

$$\frac{Q_s}{M_s}(C_{s0} - C_s) - r_{Au} = \frac{dC_s}{dt} \tag{10}$$

$$\frac{Q_l}{M_l}(C_{l0} - C_l) + \frac{M_s}{M_l}r_{Au} = \frac{dC_l}{dt} \tag{11}$$

$$\frac{Q_l}{M_l}(C_{CN0} - C_{CN}) + \frac{Q_{CN}}{M_l} - r_{CN} = \frac{dC_{CN}}{dt} \tag{12}$$

where Q_s is the solid flow rate of ore pulp; Q_l is the liquid flow rate of ore pulp; C_{s0} and C_{l0} are the initial gold concentrations of the solid and liquid, respectively; M_s is the mass of the solid ore pulp in the leaching tank; M_l is the mass of liquid ore pulp in the leaching tank; C_{CN0} is the initial cyanide ion concentration of the liquid; C_s and C_l are the concentrations of solid and liquid gold in the leaching tank, respectively; C_{CN} is the liquid cyanide ion concentration; Q_{CN} is the addition flow rate of sodium cyanide; r_{Au} is the gold dissolution rate; r_{CN} is the consumption rate of the cyanide ion.

Equations 10 and 12 can be rewritten as

$$r_{Au,i} = \frac{d\overline{C}_{s,i}}{dt} \tag{13}$$

$$r_{CN,i} = \frac{d\overline{C}_{CN,i}}{dt} \tag{14}$$

where $\overline{C}_{s,i}(0) = 0$ and $\overline{C}_{CN,i}(0) = 0$.

Generalized measurements A and B based on gold solid and liquid concentrations can be obtained by integrating both sides of eqs 13 and 14, respectively, as follows

$$\begin{aligned}\overline{C}_{s,i}(t) &= \int_0^t r_{Au,i}(t)dt \\ &= \int_0^t \left[\frac{Q_{s,i}}{M_{s,i}}(C_{s,i-1} - C_{s,i}(t)) - \frac{dC_{s,i}(t)}{dt}\right]dt \\ &= \frac{Q_{s,i}}{M_{s,i}}C_{s,i-1}t - \frac{Q_{s,i}}{M_{s,i}}\int_0^t C_{s,i}(t)dt - C_{s,i}(t) \\ &\quad + C_{s,i-1}\end{aligned} \tag{15}$$

$$\begin{aligned}\overline{C}_{CN,i}(t) &= \int_0^t r_{CN,i}(t)dt \\ &= \int_0^t \left[\frac{Q_{l,i}}{M_{l,i}}(C_{CN,i-1} - C_{CN,i}(t)) + \frac{Q_{CN,i}(t)}{M_{l,i}} \right. \\ &\quad \left. - \frac{dC_{CN,i}(t)}{dt}\right]dt \\ &= \frac{Q_{l,i}}{M_{l,i}}C_{CN,i-1}t - \frac{Q_{l,i}}{M_{l,i}}\int_0^t C_{CN,i}(t)dt \\ &\quad + \frac{1}{M_{l,i}}\int_0^t Q_{CN,i}(t)dt - C_{CN,i}(t) + C_{CN,i-1}\end{aligned} \tag{16}$$

The gold dissolution rate r_{Au} is a nonlinear function of the average diameter of ore particles $\overline{d}$, dissolved oxygen concentration C_O, liquid cyanide ion concentration C_{CN}, and solid gold concentration C_s and can be expressed as

$$r_{Au} = f(\overline{d}, C_O, C_{CN}, C_s) \tag{17}$$

The consumption rate of cyanide ion r_{CN} is a nonlinear function of the $\overline{d}$ and C_{CN}, and can be expressed by

$$r_{CN} = g(\overline{d}, C_{CN}) \tag{18}$$

The solid and liquid mass of ore pulp satisfies the conservation relation. The relationship between the solid flow rate and the liquid flow rate of ore pulp can be expressed as

$$Q_l = Q_s\left(\frac{1}{C_w} - 1\right) \tag{19}$$

where C_w is the ore pulp concentration.

The average residence time of the chemical reaction can be computed by

$$\tau = \frac{V}{\frac{Q_s}{\rho_s} + \frac{Q_l}{\rho_l}} \times 1000 \tag{20}$$

where ρ_s and ρ_l are the solid density and liquid density of the ore pulp, respectively; V is the volume of the leaching tank.

The residence mass of the solid and liquid in the leaching tank can be expressed as

$$M_s = Q_s \times \tau \tag{21}$$

$$M_l = Q_l \times \tau \tag{22}$$

The leaching rate of gold can be computed by

$$y_1 = \frac{C_{s0} - C_s}{C_{s0}} \times 100\% \tag{23}$$

The mechanism model of the leaching process is a typical nonlinear function and can be expressed as

$$\begin{aligned}y_1 = F(&C_{s0}, C_{CN0}, M_s, M_l, Q_s, Q_l, \\ &Q_{CN}, \overline{d}, C_w, V_i, \rho_s, \rho_l, C_o, r_{Au}, r_{CN})\end{aligned} \tag{24}$$

https://doi.org/10.1021/acsomega.2c06830
ACS Omega 2023, 8, 6559−6570

The leaching tank is serially connected by ore pulp overflow. The effective volume of each leaching tank is the same. It is assumed that the reactants in the leaching tank can be mixed adequately. Material isolation is neglected. The resistance of the ore pulp is constant. The input and output schematic diagram of the cascade leaching process is shown in Figure 5. For the stable operation of the leaching industrial process, according to the mass conservation principle, we get

$$Q_s = Q_{s0} \tag{25}$$

$$Q_l = Q_{l0} \tag{26}$$

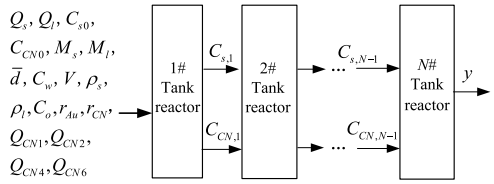

Figure 5. Input and output schematic diagram of the cascade leaching process.

The total leaching rate of the cascaded gold cyanidation leaching process can be expressed as

$$y = \frac{C_{s0} - C_{sN}}{C_{s0}} \times 100\% \tag{27}$$

where C_{sN} is the solid gold concentration of the Nth leaching tank.

The addition of sodium cyanide to each leaching tank is an operational variable. The model structure of each leaching tank in the cascade leaching process is the same, but the kinetic reaction velocity model parameters of different leaching tanks need to be estimated. If every leaching tank model adopts the same parameter, it will cause model mismatch and reduce the prediction accuracy of the leaching rate. Therefore, the unknown parameters in the model should be identified by the actual process data. The gold dissolution rate $r_{Au} = f(\overline{d}, C_O, C_{CN}, C_s)$ and the consumption rate of the cyanide ion $r_{CN} = g(\overline{d}, C_{CN})$ cannot use the detection equipment for online measurement. The key adjusting parameters u_{Au} and u_{CN} in the gold dissolution rate and cyanide ion consumption rate models need to be estimated. When estimating the unknown parameters of the dynamic model, the errors caused by model structure approximation and ideal assumptions are not considered. The mechanism model of leaching process is derived by rigorous mathematical operation. The mechanism model cannot accurately describe all characteristics and complex variable relationships of the actual process. The variation of production working conditions and random disturbance will lead to the mismatching of mechanism model parameters, which will cause a large prediction error. According to the chemical principle involved in the leaching process and the actual production demand, the sodium cyanide content of the four leaching tanks in the leaching process should satisfy the constraint requirement of gradually decrease. This production technique strategy can effectively improve the utilization efficiency of sodium cyanide and reduce environmental pollution. Therefore, the leaching process control input signal should satisfy the following constraints.

$$Q_{CN_1} > Q_{CN_2} > Q_{CN_4} > Q_{CN_6} \tag{28}$$

4. MODEL-FREE ADAPTIVE CONTROL OF THE LEACHING PROCESS

The theoretical basis of MFAC control is the general model, which dynamically linearizes and controls the nonlinear system. The discrete-time control multiple input single output (MISO) system can be expressed as

$$y(k+1) = f(y(k), \cdots, y(k-n_y), \boldsymbol{u}(k), \cdots, \boldsymbol{u}(k-n_u)) \tag{29}$$

where $\boldsymbol{u}(k) \in \boldsymbol{R}^m$ and $y(k) \in \boldsymbol{R}$, respectively, represent the input and output of the system at time k; n_u and n_y are the orders of the input and output of the system, respectively; $f(\cdots) \in \prod_{n_y+1} \boldsymbol{R} \times \prod_{n_u+1} \boldsymbol{R}^{\boldsymbol{m}} \to \boldsymbol{R}$ is an unknown nonlinear function.

Without loss of generality, the following assumptions are taken.

Assumption 1: $f(\cdots)$ is a continuous partial derivative with respect to each component of the $(n+2)$th variable.

Assumption 2: System (29) satisfies the generalized Lipschitz condition, which means, for any $k_1 \neq k_2$, $k_1, k_2 \geq 0$ and $u(k_1) \neq u(k_2)$, we have

$$|y(k_1+1) - y(k_2+1)| \leq b\|\boldsymbol{u}(k_1) - \boldsymbol{u}(k_2)\| \tag{30}$$

where $y(k_i+1) = f(y(k_i), \cdots, y(k_i-n_y), \boldsymbol{u}(k_i), \cdots, \boldsymbol{u}(k_i-n_u))$; b_i, $i = 1,2 > 0$ is a constant.

For the MISO discrete-time nonlinear system satisfying the assumptions 1 and 2 above, for $\|\boldsymbol{u}(k)\| \neq 0$, there must be a time-varying parameter vector $\phi(k) \in \boldsymbol{R}^m$, so that the system (29) can be transformed into the following CFDL data model.

$$\Delta y(k+1) = \Phi^T(k)\Delta\boldsymbol{u}(k) \tag{31}$$

where $\Phi(k) = [\phi_1(k), \phi_2(k), \cdots, \phi_m(k)]^T$ is bounded for any time k.

Eq 31 is a general model, in which $\phi(k)$ is the PG of the system. Using eq 31, eq 29 can be linearized to obtain the following expression

$$y(k+1) = y(k) + \Phi^T(k)\Delta\boldsymbol{u}(k) \tag{32}$$

By transforming the complex chemical leaching system into a multiparameter linear time-varying system, the MFAC controller can be designed theoretically.

Consider the following control input criterion function.

$$J(\boldsymbol{u}(k)) = \left\|y_d(k+1) - y(k+1)\right\|^2 + \beta\|\boldsymbol{u}(k) - \boldsymbol{u}(k+1)\|^2 \tag{33}$$

where $\beta > 0$ is the weight factor, which is used to control for excessive changes in the input; $y_d(k+1)$ is the expectation output signal.

Substituting eq 32 into eq 33 and differentiating with respect to $\boldsymbol{u}(k)$, for $\partial J(\boldsymbol{u}(k))/\partial\boldsymbol{u}(k) = 0$, the following control law can be obtained.

https://doi.org/10.1021/acsomega.2c06830
ACS Omega 2023, 8, 6559−6570

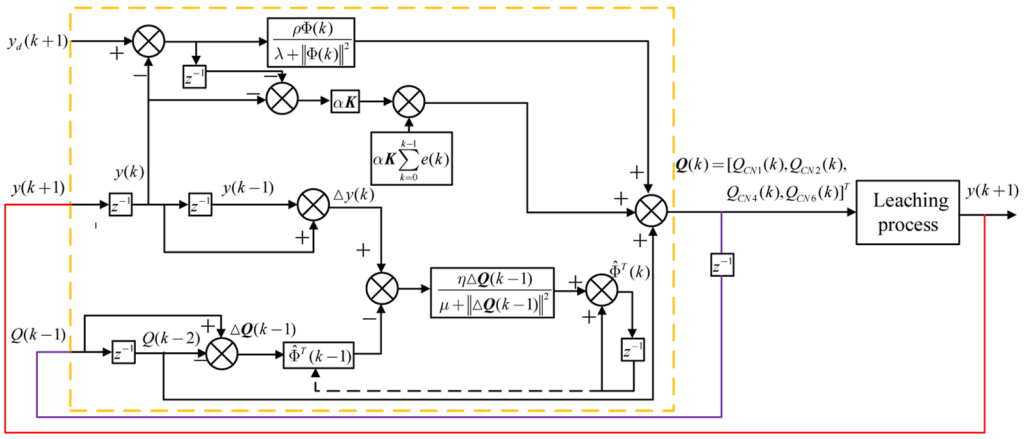

Figure 6. Schematic diagram of ICFDL-MFAC controller for the leaching process.

$$\boldsymbol{u}(k) = \boldsymbol{u}(k-1) + \frac{\rho\Phi(k)(y_{\mathrm{d}}(k+1) - y(k))}{\lambda + \|\Phi(k)\|^2} \tag{34}$$

where $\rho \in (0,1]$ is the step factor; λ is the control parameter of the control law. The PG $\Phi(k)$ changes with the input and output data.

When the state of the system at different moments is known, the expectation output $y_{\mathrm{d}}(k+1)$ of the system can be obtained by the MFAC controller. For the complex chemical leaching system, in order to obtain faster control rate and better accuracy, the following control law with integral term is constructed

$$\boldsymbol{Q}(k) = \boldsymbol{Q}(k-1) + \frac{\rho\hat{\Phi}(k)(y_{\mathrm{d}}(k+1) - y(k))}{\lambda + \|\hat{\Phi}(k)\|^2} + \boldsymbol{K}\sum_{j=1}^{k} e(j) \tag{35}$$

where $e(j) = y_{\mathrm{d}}(j) - y(j)$ is the output tracking error; $\boldsymbol{K} = [K_1, K_2, \cdots, K_i]$ is the integral proportionality coefficient.

In order to prevent the phenomenon of integral saturation, the integral control factor α is introduced to obtain the following control law with anti-integral saturation ability.

$$\boldsymbol{Q}(k) = \boldsymbol{Q}(k-1) + \frac{\rho\hat{\Phi}(k)(y_{\mathrm{d}}(k+1) - y(k))}{\lambda + \|\hat{\Phi}(k)\|^2} + \alpha\boldsymbol{K}\sum_{j=1}^{k} e(j) \tag{36}$$

$$\alpha = \begin{cases} 1, & |e(k)| \geq \varepsilon \\ 0, & |e(k)| < \varepsilon \end{cases} \tag{37}$$

The parameter estimation algorithm derived from the minimization criterion function constructed by the square of the difference between the system model output and the real output is too sensitive to inaccurate sampled data. There are nonlinear uncertainties in the chemical leaching system. In order to ensure the rate of change of the PG, the following criterion function is taken.

$$J(\Phi(k)) = \|y(k) - y(k-1) - \Phi^T(k)\Delta\boldsymbol{u}(k-1)\|^2 + \mu\|\Phi(k) - \hat{\Phi}(k-1)\|^2 \tag{38}$$

For $\partial J(\Phi(k))/\partial\hat{\Phi}(k) = 0$, the PG estimation law can be obtained as follows

$$\hat{\Phi}(k) = \hat{\Phi}(k-1) + \frac{\eta\Delta\boldsymbol{u}(k-1)(\Delta y(k) - \hat{\Phi}^T(k-1)\Delta\boldsymbol{u}(k-1))}{\mu + \|\Delta\boldsymbol{u}(k-1)\|^2} \tag{39}$$

where $\eta \in (0,2]$ is the step factor; $\mu > 0$ is the weighting factor, which is used to penalize large changes in the PG estimation. The estimation of the PG will change with the actual input and output, which can reduce the influence of system disturbance on the PG, so as to ensure the accuracy of the controller.

The general model of the chemical leaching system replaces the mechanism model of the chemical leaching system as follows

$$y(k+1) = f(y(k), \cdots, y(k-n_y), \boldsymbol{Q}(k), \cdots, \boldsymbol{Q}(k-n_{\mathrm{q}})) \tag{40}$$

where $y(k)$ is the leaching rate; $\boldsymbol{Q}(k) = [Q_{\mathrm{CN1}}(k), Q_{\mathrm{CN2}}(k), Q_{\mathrm{CN4}}(k), Q_{\mathrm{CN6}}(k)]^T$ is sodium cyanide addition variable of the four leaching tanks; n_y and n_q is the order of the system output and input.

According to eqs 34 and 39, the control scheme of MFAC for the chemical leaching system can be obtained as follows

$$\hat{\Phi}(k) = \hat{\Phi}(k-1) + \frac{\eta\Delta\boldsymbol{Q}(k-1)(\Delta y(k) - \hat{\Phi}^T(k-1)\Delta\boldsymbol{Q}(k-1))}{\mu + \|\Delta\boldsymbol{Q}(k-1)\|^2} \tag{41}$$

$\hat{\phi}_i(k)$ is taken as $\hat{\phi}_i(k) = \hat{\phi}_i(1)$, for $|\hat{\phi}_i(k)| < \varepsilon$ or

$$\mathrm{sign}(\hat{\phi}_i(k)) \neq \mathrm{sign}(\hat{\phi}_i(1)),\ i = 1,2,3,4 \tag{42}$$

https://doi.org/10.1021/acsomega.2c06830
ACS Omega 2023, 8, 6559−6570

$$\boldsymbol{Q}(k) = \boldsymbol{Q}(k-1) + \frac{\rho\hat{\Phi}(k)(y_d(k+1) - y(k))}{\lambda + \|\hat{\Phi}(k)\|^2} + \alpha\boldsymbol{K}\sum_{j=1}^{k} e(j) \tag{43}$$

$$\alpha = \begin{cases} 1, & |e(k)| \geq \varepsilon \\ 0, & |e(k)| < \varepsilon \end{cases} \tag{44}$$

where $\lambda > 0$; $\mu > 0$; $\eta \in (0,2]$; $\rho \in (0,1]$; $\hat{\Phi}(k) = [\phi_1(k), \phi_2(k), \phi_3(k), \phi_4(k)]^T \in \boldsymbol{R}^4$ is the estimation of the PG $\Phi(k)$; The initial value of $\hat{\phi}_i(k)$ is taken $\hat{\phi}_i(k) = \hat{\phi}_i(1)$, $i = 1,2,3,4$; $y_d(k+1)$ is the expectation leaching rate; $\Delta y(k) = y(k) - y(k-1)$; $\boldsymbol{K} = [K_1,K_2,K_3,K_4]$ is the integral proportionality coefficient; $\Delta\boldsymbol{Q}(k-1) = \boldsymbol{Q}(k-1) - \boldsymbol{Q}(k-2)$.

Eq 42 is the reset mechanism of the PG estimation law, which is introduced to make the PG estimation algorithm have stronger tracking ability for time-varying parameters. The MFAC control structure of the leaching process is determined by eqs 41 and 43, and its internal structure is shown in Figure 6. The control output of the next moment is obtained from the expected input signal, output signal, and control quantity of the previous moment. The proposed model-free adaptive control algorithm based on compact form dynamic linearization with integration term is named as ICFDL-MFAC.

In order to ensure that the control algorithm satisfies the input variable constraints of the leaching process as shown in eq 28, by combining eqs 43 and 44, we have

$$\Delta\boldsymbol{Q}(k) = \frac{\rho\hat{\Phi}(k)(y_d(k+1) - y(k))}{\lambda + \|\hat{\Phi}(k)\|^2} + \alpha\boldsymbol{K}\sum_{j=1}^{k} e(j) \tag{45}$$

$y_d(k+1) - y(k)$, $\|\hat{\Phi}(k)\|$, and $\alpha\sum_{j=1}^{k} e(j)$ are constants for every definite time k. Therefore, the inputs of the four leaching tanks are only related to $\hat{\Phi}(k)$ and $\boldsymbol{K}$. According to eq 41, it can be seen that for each determined time k, the change magnitude of the PG corresponding to the four input quantities in $\hat{\Phi}(k)$ is only related to $\hat{\Phi}(k-1)$ and $\Delta\boldsymbol{Q}(k-1)$ because the change amplitude of the four input variables in $\Delta\boldsymbol{Q}(k-1)$ is only related to $\hat{\Phi}(k-1)$ and $\boldsymbol{K}$. Therefore, the PGs in $\hat{\Phi}(k)$ corresponding to the four input variables are only related to $\hat{\Phi}(k-1)$ and $\boldsymbol{K}$. Therefore, when $\hat{\Phi}(1)$ and $\boldsymbol{K}$ are initialized to satisfy the following inequalities, the input variables in the leaching process can satisfy the constraints of eq 28 in the adaptive control update process.

$$\begin{cases} \phi_1(1) \geq \phi_2(1) \geq \phi_3(1) \geq \phi_4(1) \\ K_1 \geq K_2 \geq K_3 \geq K_4 \end{cases} \tag{46}$$

5. CONVERGENCE ANALYSIS OF THE ICFDL-MFAC ALGORITHM

In order to research the convergence and stability of the ICFDL-MFAC control system, the following assumption 3 is taken.

Assumption 3: The symbols of the elements in the PG remain the same.

The convergence of the ICFDL-MFAC algorithm is illustrated in Theorem 1.

Theorem 1: For the ICFDL-MFAC algorithm composed of eqs 41−43, when it satisfies the assumptions 1, 2, and 3 and the expectation output $y_d(k+1)$ is constant, if η, μ and λ are taken appropriate values, there will be a positive number $\lambda_{min} > 0$. When λ satisfies $\lambda \geq \lambda_{min}$, the control algorithm satisfies the following conclusions.

(1) The output tracking error is convergent, that is, $\lim_{k\to\infty} |y(k+1) - y_d(k+1)| = 0$;

(2) The output sequence $\{y(k)\}$ and input sequence $\{\boldsymbol{Q}(k)\}$ of the system are bounded

Proof: The variation between the estimation and the true value of $\Phi(k)$ is defined as

$$\tilde{\Phi}(k) = \hat{\Phi}(k) - \Phi(k) \tag{47}$$

From eq 41, we have

$$\tilde{\Phi}(k) = \hat{\Phi}(k-1) - \Phi(k) + \frac{\eta\Delta\boldsymbol{Q}(k-1)(\Delta y(k) - \hat{\Phi}^T(k-1)\Delta\boldsymbol{Q}(k-1))}{\mu + \|\Delta\boldsymbol{Q}(k-1)\|^2} \tag{48}$$

Substituting eq 31 into eq 48, the following equation can be obtained from eq 30 as

$$\|\Phi(k)\| \leq \left\| \boldsymbol{I} - \frac{\eta\Delta\boldsymbol{Q}(k-1)\Delta\boldsymbol{Q}^T(k-1)}{\mu + \|\Delta\boldsymbol{Q}(k-1)\|^2} \right\| \|\Phi(k-1)\| + 2b \tag{49}$$

where b is an appropriate constant.

For $\mu > 0$, $\eta \in (0,2]$, we can obtain the following equation

$$0 < \left\| \boldsymbol{I} - \frac{\eta\Delta\boldsymbol{Q}(k-1)\Delta\boldsymbol{Q}^T(k-1)}{\mu + \|\Delta\boldsymbol{Q}(k-1)\|^2} \right\| \leq d < 1 \tag{50}$$

Substituting eq 50 into eq 49, the following inequality can be obtained

$$\begin{aligned} \|\tilde{\Phi}(k)\| &\leq d\|\tilde{\Phi}(k-1)\| + 2b \\ &\leq d^2\|\tilde{\Phi}(k-2)\| + 2db + 2b \\ &\leq \cdots \leq d^{k-1}\|\tilde{\Phi}(1)\| + \frac{2b}{1-d} \end{aligned} \tag{51}$$

According to eq 51, when $d < 1$, $\|\tilde{\Phi}(k)\|$ is bounded, and since $\Phi(k)$ is bounded, $\hat{\Phi}(k)$ is also bounded.

The output error of the system is defined as $e(k) = y_d - y(k)$, and combining eqs 31 and 43, the following equation can be obtained

$$e(k+1) = \left[1 - \frac{\rho\Phi(k)\hat{\Phi}^T(k)}{\lambda + \|\hat{\Phi}(k)\|^2}\right] e(k) \tag{52}$$

According to the reset algorithm of eq 42 and assumption 3, $\phi_i(k)\hat{\phi}_i(k) > 0$, $i = 1,2,3,4$ can be obtained.

Then there exists appropriate ρ and λ that satisfy the following equation

https://doi.org/10.1021/acsomega.2c06830
ACS Omega 2023, 8, 6559−6570

$$0 < \left| 1 - \frac{\rho \Phi(k) \hat{\Phi}^T(k)}{\lambda + \|\hat{\Phi}(k)\|^2} \right| = \left| 1 - \frac{\rho \sum_{i=1}^{4} \phi_i(k) \hat{\phi}_i(k)}{\lambda + \|\hat{\Phi}(k)\|^2} \right| \leq 1 - \rho M < 1 \tag{53}$$

Taking $f = 1 - \rho M$ and combining eqs 52 and 53, the following equation can be derived

$$|e(k+1)| \leq f|e(k)| \leq f^2|e(k-1)| \leq \cdots \leq f^k|e(k)| \tag{54}$$

From eq 54, we can obtain $\lim_{k\to\infty} |y(k+1) - y_d(k+1)| = 0$, and thus the conclusion (1) of Theorem 1 can be proved. By the convergence of the output tracking error $e(k)$ and the boundedness of the expectation output, it can be concluded that $y(k)$ is bounded.

Since $\hat{\Phi}(k)$ is bounded, it is always possible to find a positive number N such that the following equation holds

$$\left\| \frac{\rho \hat{\Phi}^T(k)}{\lambda + \|\hat{\Phi}(k)\|^2} \right\| \leq \mathrm{N} \tag{55}$$

Combining eqs 43, 54, and 55, we have

$$\begin{aligned}
\|\boldsymbol{Q}(k)\| &\leq \|\boldsymbol{Q}(k) - \boldsymbol{Q}(k-1)\| + \|\boldsymbol{Q}(k-1)\| \\
&\leq \|\boldsymbol{Q}(k) - \boldsymbol{Q}(k-1)\| + \|\boldsymbol{Q}(k-1) - \boldsymbol{Q}(k-2)\| + \|\boldsymbol{Q}(k-2)\| \\
&\leq \|\Delta \boldsymbol{Q}(k)\| + \|\Delta \boldsymbol{Q}(k-1)\| + \cdots + \|\Delta \boldsymbol{Q}(1)\| + \|\boldsymbol{Q}(0)\| \\
&\leq N(e(k) + \alpha \|\boldsymbol{K}\| \left(\sum_{j=0}^{k} e(j) + \sum_{j=0}^{k-1} e(j) + \cdots + e(1) \right) + \|\boldsymbol{Q}(0)\| \\
&\leq N(f^{k-1} + f^{k-2} + \cdots + f + 1)e(1) + \alpha \|\boldsymbol{K}\| [N(f^{k-1} + f^{k-2} + \cdots + f + 1) e(1) \\
&\quad + N(f^{k-2} + \cdots + f + 1)e(1) + \cdots + e(1)] + \|\boldsymbol{Q}(0)\| \\
&\leq [N(f^{k-1} + f^{k-2} + \cdots + f + 1) + \alpha \|\boldsymbol{K}\| (N(f^{k-1} + f^{k-2} + \cdots + f + 1) \\
&\quad + N(f^{k-2} + \cdots + f + 1) + \cdots + 1)] e(1) + \|\boldsymbol{Q}(0)\|
\end{aligned} \tag{56}$$

According to eq 53, the control input $\boldsymbol{Q}(k)$ is bounded, which also proves that the ICFDL-MFAC controller is convergent and stable.

6. EXPERIMENTAL VERIFICATION

For the chemical leaching system, the output leaching rate can be controlled by controlling the amount of NaCN added to the four leaching tanks. The variables and parameter values involved in the leaching system are shown in Table 1. The

Table 1. Variables and Value in the Mechanistic Model

variables	value	unit
C_w	39	%
C_{w0}	0	mg/kg
C_s	5	mg/kg
C_l	0	mg/kg
C_O	7	mg/kg
$\overline{d}$	80	μm
C_{CN0}	250	mg/kg
Q_s	2500	kg/h
V	68	m^3
ρ_s	2.8	g/cm^3
ρ_l	1	g/cm^3

detailed system parameters are shown in refs 7 and 8. The sampling period of the system is 200 s. The time-varying target leaching rate of the chemical leaching system output is taken as

$$y_d = \begin{cases} 0.93, 0 < k \leq 500 \\ 0.97, 501 < k \leq 1000 \\ 0.95, 1001 < k \leq 1500 \end{cases} \tag{57}$$

The initial values of the proposed ICFDL-MFAC control algorithm are taken as $y(0) = 0$, $\boldsymbol{Q}(0) = [0,0,0,0]^T$, $\hat{\Phi}(0) = [20,10,5,0.5]^T$, $\rho = 1$, $\eta = 2$, $\mu = 0.8$, $\lambda = 0.001$, $\varepsilon = 0.0001$, $\boldsymbol{K}_{\mathrm{MFAC}} = [0.5,0.5,0.3,0.2]$. In order to compare and highlight the advantages of the proposed algorithm, the CFDL-MFAC without integration term algorithm in ref 24, the existing difference estimator algorithm based on CFDL-MFAC (DECFDL-MAFC) in ref 25, and the control algorithm proposed in the ref 39 named as Meng are also verified. The adaptive control strategy based on the RBF neural network with integration term in ref 40 is named as IRBF and also tested for comparison. The control parameters in the IRBF algorithm are taken as $\gamma = 0.01$ and $\sigma = 0.001$. The structure of IRBF neural network contains nine hidden layers. The control inputs of the RBF neural network are taken as $z(k) = y(k)$, $c_i = [-2,-1.5,-1.0,-0.5,0,0.5,1.0,1.5,2]^T$,and $b_i = 3$. The initial values of the weights of the RBF neural network are taken as $\omega_2 = [0.9,0.6,0.4,0.3]\omega_1 = [1,0.7,0.5,0.4]$, $\omega_3 = [0.8, 0.5, 0.3, 0.2]$, and $\omega = [\omega_1; \omega_2; \omega_3; \omega_1; \omega_2; \omega_3; \omega_1; \omega_2; \omega_3]$. The proportional coefficient of RBF neural network is taken as $\boldsymbol{K}_{\mathrm{RBF}} = [5,5,3,2]$. The dynamic control results of the target leaching rate based on the different control algorithms are shown in the Figure 7. The dynamic variations of the four leaching tanks in the leaching process based on the different control algorithms are shown in Figure 8. The control output errors of the different adaptive control algorithms are shown in Figure 9.

For the systems with multiple input and single output, the update of the PG of the MFAC algorithm and the update of the control law are achieved driven by the output tracking error. For chemical leaching processes, the amount of change in the control input and output varies greatly in terms of dimensions. In the control process, the numerical change of the leaching rate is very small and slow. Especially when the set control output value reaches a certain value, the change of the leaching rate is too small or even difficult to drive the control

https://doi.org/10.1021/acsomega.2c06830
ACS Omega 2023, 8, 6559−6570

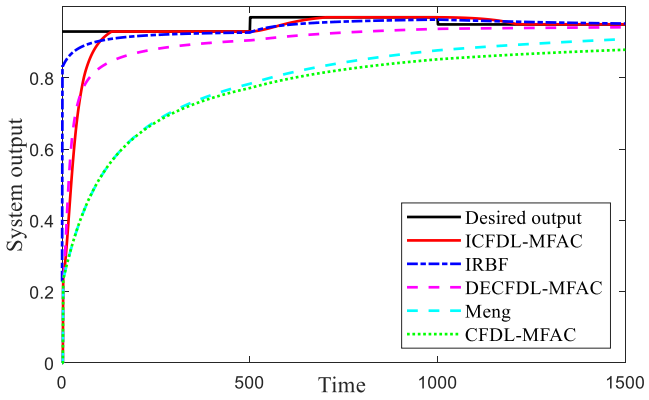

Figure 7. Leaching rate dynamic tracking results of different control algorithms.

input change. Besides, the control input changes several times and the control output may be almost constant. Therefore, for the MFAC algorithm without the integration term, the updates of its PG and control law cannot quickly meet the actual needs of the system and thus cannot achieve effective control tracking. For the DECFDL-MFAC algorithm, its error amplification term is added to the PG update and the control law update, which is better than CFDL-MFAC and Meng's control algorithm. However, the error amplification capability of the DECFDL-MFAC algorithm is far from enough compared with the ICFDL-MFAC algorithm.

In order to quantify the control accuracy of different control algorithms, the mean error of the control output error is defined as $y_{\mathrm{err}} = \left[\sum_{i=1}^{N} (y_{\mathrm{d}}(i) - y(i))\right]/N$. The mean error of the control output error based on different control algorithms is shown in Table 2.

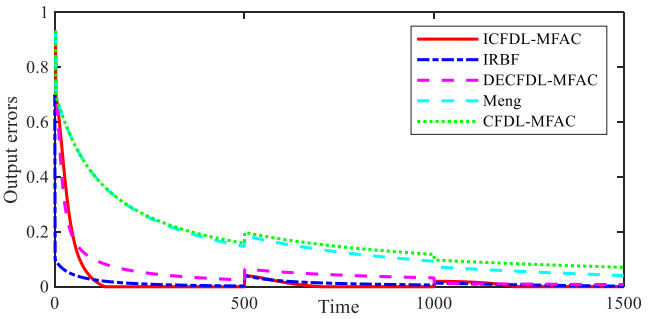

Figure 9. Control output errors based on different adaptive control algorithms.

7. RESULTS AND DISCUSSION

From the above experimental verification control results, it can be seen that the mean error of the proposed control algorithm is 0.0136, which is much smaller than that of other control algorithms. The rise time or peak time is usually used to evaluate the response speed of the system. For the system in this paper, the rise time is selected to evaluate the response speed of the system. The rise time refers to the time required for the response curve to rise from zero to 90% of the steady-state value for the first time. The rise time of the other three control algorithms is shown in Table 3. It can be seen from Figure 7 that the traditional CFDL-MFAC, DECFDL-MFAC, and Meng's control algorithm cannot meet the conditions for calculating the rise time in the control process. Therefore, the rise time of the two control algorithms is not given. We can see that although the proposed ICFDL-MFAC method does not have the smallest rise time, it is the most stable and accurate.

It can be seen that the dynamic control inputs of the MFAC control algorithm and the IRBF control algorithm are smooth. However, under the same control conditions, the response speed of the control input based on MFAC is faster than that

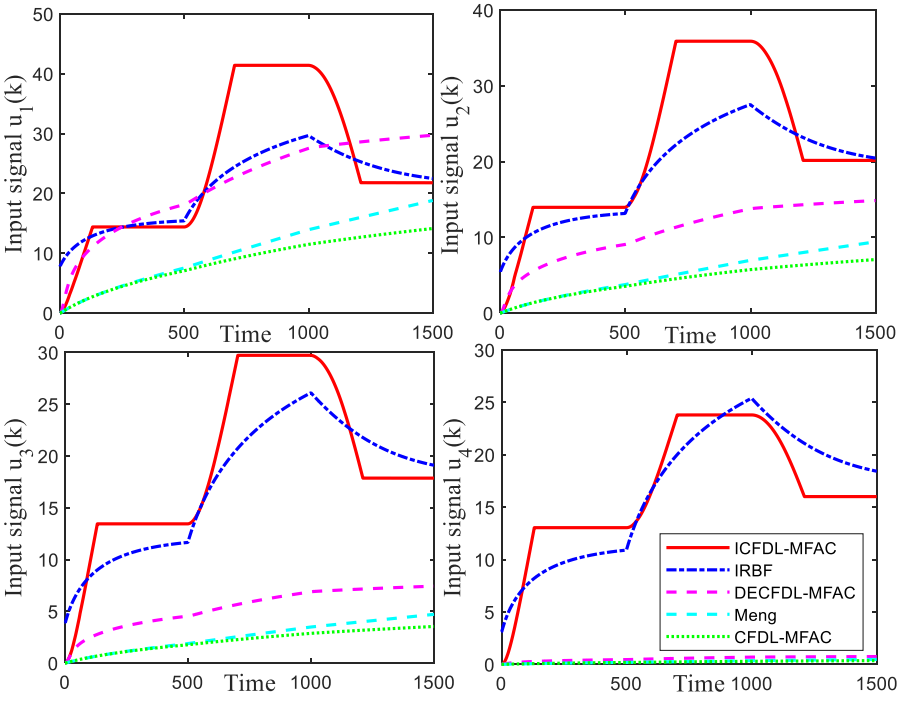

Figure 8. Dynamic input of four leaching tanks based on different control algorithms.

https://doi.org/10.1021/acsomega.2c06830
ACS Omega 2023, 8, 6559−6570

Table 2. Mean Error of the Control Output Error Based on Different Control Algorithms

	ICFDL-MFAC	IRBF	DECFDL-MFAC	Meng	CFDL-MFAC
mean error	0.0136	0.0227	0.0484	0.1622	0.1793

Table 3. Rise Times Based on Different Algorithms

	ICFDL-MFAC	IRBF	DECFDL-MFAC
rise times (s)	13,800	1000	23,000

IRBF control algorithm. The weight updating strategy of the IRBF control algorithm has a limitation. When the output feedback error is less than a certain threshold, the weight will not be updated. The IRBF control algorithm involves more regulation parameters and has higher control complexity. The IRBF control algorithm is difficult to satisfy the actual four inputs constraints of production. Therefore, the precision adjustment of the IRBF control algorithm is more difficult, which limits its application and implementation in the hydrometallurgical leaching process of precious gold. In contrast, the MFAC control algorithm involves fewer control adjustment parameters and has better accuracy and stationarity. By adding integral weights to the input variables, the proposed control algorithm based on MFAC not only achieves the expectation leaching rate but also achieves the production requirement that the input sodium cyanide content of the four leaching tanks is gradually decreasing. The proposed control algorithm can easily adjust the input constraints proportionally according to the production requirements. The MFAC control algorithm can effectively track the dynamic changes of the target leaching rate.

8. CONCLUSIONS

The cascade leaching process of hydrometallurgy involves many complex multiphase chemical reaction principles and physical conservation principles. The cascade leaching process model involves many undetermined parameters and assumptions. It is difficult and computationally complex to establish an accurate mechanism model for predicting the leaching rate. Imprecise prediction model may degrade the performance of model-based control strategies. Model-free adaptive control strategy has its unique adaptability and advantages in controlling the complex cascade leaching process. There are process constraints and limitations among the input variables in the actual cascade leaching process. In order to solve the constraint problem between input variables, a novel model-free adaptive control algorithm has been designed by introducing the integral factor parameter of input variables. By setting the initial value of the input to the PG and the weight of the integral coefficient, the input variable constraint can be adjusted and satisfied adaptively. According to scientific assumptions, the stability convergence of the model-free adaptive control algorithm is analyzed and proved. Based on the data sampled from the leaching industrial process, the superiority and practicability of the proposed model-free adaptive control algorithm are verified by comparing with the existing model-free control method. The main advantages of MFAC include the ability to accurately control a system using only the input and output data of the system. Compared with the PID control algorithm, the MFAC algorithm can easily realize the precise control of the MIMO system. Compared with the neural network and other intelligent control algorithms, the MFAC algorithm has the advantages of simple structure and small computation burden. However, some parameters of the MFAC control algorithm need to be adjusted, which takes a little time when applied to the industrial system. The standard MFAC algorithm is difficult to achieve a good control of the integral system. The existing MFAC control algorithm can be improved to apply to time-delay systems and output constrained systems. The MFAC algorithm may be optimized to reduce the workload of adjusting parameters in engineering applications. The MFAC algorithm can also be applied to control MIMO of other chemical processes, power systems, or mechanical systems.

AUTHOR INFORMATION

Corresponding Author

Shijian Dong − *Engineering Research Center of Intelligent Control for Underground Space, Ministry of Education, China University of Mining and Technology, Xuzhou 221116, China; School of Information and Control Engineering, China University of Mining and Technology, Xuzhou 221116, China;* orcid.org/0000-0001-6635-9081; Email: dsjggy@126.com

Authors

Yuzhu Zhang − *Engineering Research Center of Intelligent Control for Underground Space, Ministry of Education, China University of Mining and Technology, Xuzhou 221116, China; School of Information and Control Engineering, China University of Mining and Technology, Xuzhou 221116, China*

Xingxing Zhou − *Engineering Research Center of Intelligent Control for Underground Space, Ministry of Education, China University of Mining and Technology, Xuzhou 221116, China; School of Information and Control Engineering, China University of Mining and Technology, Xuzhou 221116, China*

Dapeng Niu − *College of Information Science and Engineering, Northeastern University, Shenyang 110819, China*

Xuesong Wang − *Engineering Research Center of Intelligent Control for Underground Space, Ministry of Education, China University of Mining and Technology, Xuzhou 221116, China; School of Information and Control Engineering, China University of Mining and Technology, Xuzhou 221116, China*

Complete contact information is available at: https://pubs.acs.org/10.1021/acsomega.2c06830

Notes

The authors declare no competing financial interest.

ACKNOWLEDGMENTS

The work was supported by the Fundamental Research Funds for the Central Universities under grant no. 2022QN1048.

REFERENCES

(1) Jia, R.; You, F. Multi-stage economic model predictive control for a gold cyanidation leaching process under uncertainty. *AIChE J.* **2021**, *67*, No. e17043.

https://doi.org/10.1021/acsomega.2c06830
ACS Omega 2023, 8, 6559−6570

(2) Jha, M. K.; Kumari, A.; Panda, R.; Rajesh Kumar, J. R.; Yoo, K.; Lee, J. Y. Review on hydrometallurgical recovery of rare earth metals. *Hydrometallurgy* **2016**, *165*, 2−26.
(3) Barragan, J. A.; Ponce de León, C.; Alemán Castro, J. R.; Peregrina-Lucano, A.; Gómez-Zamudio, F.; Larios-Durán, E. R. Copper and antimony recovery from electronic waste by hydrometallurgical and electrochemical techniques. *ACS Omega* **2020**, *5*, 12355−12363.
(4) Liu, Z.; Nueraihemaiti, A.; Chen, M.; Du, J.; Fan, X.; Tao, C. Hydrometallurgical leaching process intensified by an electric field for converter vanadium slag. *Hydrometallurgy* **2015**, *155*, 56−60.
(5) Panda, R.; Dinkar, O. S.; Kumari, A.; Gupta, R.; Jha, M. K.; Pathak, D. D. Hydrometallurgical processing of waste integrated circuits (ICs) to recover Ag and generate mix concentrate of Au, Pd and Pt. *J. Ind. Eng. Chem.* **2021**, *93*, 315−321.
(6) Jia, R.; Zhang, S.; You, F. Transfer learning for end-product quality prediction of batch processes using domain-adaption joint-Y PLS. *Comput. Chem. Eng.* **2020**, *140*, 106943.
(7) Niu, D.; Liu, X.; Liu, Y.; Jia, M. Optimization control of hydrometallurgical leaching process based on IDE-MPC. *Miner. Eng.* **2022**, *176*, 107341.
(8) Zhang, J.; Tan, Y.; Li, S.; Wang, Y.; Jia, R. Comparison of alternative strategies estimating the kinetic reaction rate of the gold cyanidation leaching process. *ACS Omega* **2019**, *4*, 19880−19894.
(9) Zhang, S.; Jia, R.; He, D.; Chu, F.; Mao, Z. A general data-driven nonlinear robust optimization framework based on statistic limit and principal component analysis. *Comput. Chem. Eng.* **2022**, *160*, 107707.
(10) Hao, J.; Wang, X.; Wang, Y.; Wu, Y.; Guo, F. Optimizing the leaching Parameters and Studying the kinetics of Copper Recovery from Waste Printed Circuit Boards. *ACS Omega* **2022**, *7*, 3689−3699.
(11) Yan, H.; Wang, F.; He, D.; Wang, Q. An operational adjustment framework for a complex industrial process based on hybrid Bayesian network. *IEEE Trans. Autom. Sci. Eng.* **2020**, *17*, 1699−1710.
(12) Fisher, O. J.; Watson, N. J.; Escrig, J. E.; Witt, R.; Porcu, L.; Bacon, D.; Gomes, R. L. Considerations, challenges and opportunities when developing data-driven models for process manufacturing systems. *Comput. Chem. Eng.* **2020**, *140*, 106881.
(13) Li, Y.; Xiao, P.; Wang, Y.; Hao, Y. Mechanisms and control measures of mature biofilm resistance to antimicrobial agents in the clinical context. *ACS Omega* **2020**, *5*, 22684−22690.
(14) Chen, S. W.; Wang, T.; Atanasov, N.; Kumar, V.; Morari, M. Large scale model predictive control with neural networks and primal active sets. *Automatica* **2022**, *135*, 109947.
(15) Liu, D.; Yang, G. H. Neural network-based event-triggered MFAC for nonlinear discrete-time processes. *Neurocomputing* **2018**, *272*, 356−364.
(16) Åström, K. J.; Hang, C. C.; Persson, P.; Ho, W. K. Towards intelligent PID control. *Automatica* **1992**, *28*, 1−9.
(17) Azizitorghabeh, A.; Mahandra, H.; Ramsay, J.; Ghahreman, A. Gold leaching from an oxide ore using thiocyanate as a lixiviant: process optimization and kinetics. *ACS Omega* **2021**, *6*, 17183−17193.
(18) Jiang, Y.; Fan, J.; Chai, T.; Li, J.; Lewis, F. L. Data-driven flotation industrial process operational optimal control based on reinforcement learning. *IEEE Trans. Ind. Inf.* **2018**, *14*, 1974−1989.
(19) Zhu, S.; Liu, D.; Yang, C.; Fu, J. Synchronization of memristive complex-valued neural networks with time delays via pinning control method. *IEEE Trans. Cybern.* **2020**, *50*, 3806−3815.
(20) Rovithakis, G. A.; Christodoulou, M. A. *Adaptive Control with Recurrent High-Order Neural Networks: Theory and Industrial Applications*; Springer Science & Business Media Verlag: London, 2012; pp 1−193.
(21) Peng, H.; Ozaki, T.; Toyoda, Y.; Shioya, H.; Nakano, K.; Haggan-Ozaki, V.; Mori, M. RBF-ARX model-based nonlinear system modeling and predictive control with application to a NOx decomposition process. *Control Eng. Pract.* **2004**, *12*, 191−203.
(22) Liu, D.; Yang, G. H. Prescribed performance model-free adaptive integral sliding mode control for discrete-time nonlinear systems. *IEEE Trans. Neural Netw. Learn. Syst.* **2019**, *30*, 2222−2230.
(23) Spall, J. C.; Cristion, J. A. Model-free control of nonlinear stochastic systems with discrete-time measurements. *IEEE Trans. Autom. Control* **1998**, *43*, 1198−1210.
(24) Xu, D.; Jiang, B.; Shi, P. A novel model-free adaptive control design for multivariable industrial processes. *IEEE Trans. Ind. Electron.* **2014**, *61*, 6391−6398.
(25) Hou, Z.; Zhu, Y. Controller-dynamic-linearization-based model free adaptive control for discrete-time nonlinear systems. *IEEE Trans. Ind. Inf.* **2013**, *9*, 2301−2309.
(26) Tutsoy, O.; Barkana, D. E.; Tugal, H. Design of a completely model free adaptive control in the presence of parametric, non-parametric uncertainties and random control signal delay. *ISA Trans.* **2018**, *76*, 67−77.
(27) Zhu, Y.; Hou, Z.; Qian, F.; Du, W. Dual RBFNNs-based model-free adaptive control with aspen HYSYS simulation. *IEEE Trans. Neural Netw. Learn. Syst.* **2017**, *28*, 759−765.
(28) dos Santos Coelho, L.; Coelho, A. A. R. Model-free adaptive control optimization using a chaotic particle swarm approach. *Chaos, Solitons Fractals* **2009**, *41*, 2001−2009.
(29) Chen, C.; Lu, J. Different-factor compact-form model-free adaptive control with neural networks for MIMO nonlinear systems. *Asian J. Control* **2022**, *24*, 1688−1699.
(30) Hui, Y.; Chi, R.; Huang, B.; Hou, Z.; Jin, S. Observer-based sampled-data model-free adaptive control for continuous-time nonlinear nonaffine systems with input rate constraints. *IEEE Trans. Syst. Man Cybern. Syst.* **2021**, *51*, 7813−7822.
(31) Zhang, X.; Wang, H.; Tian, Y.; Peyrodie, L.; Wang, X. Model-free based neural network control with time-delay estimation for lower extremity exoskeleton. *Neurocomputing* **2018**, *272*, 178−188.
(32) He, W.; Chen, Y.; Yin, Z. Adaptive neural network control of an uncertain robot with full-state constraints. *IEEE Trans. Cybern.* **2016**, *46*, 620−629.
(33) Chen, M.; Ge, S. S.; How, B. V. E. Robust adaptive neural network control for a class of uncertain MIMO nonlinear systems with input nonlinearities. *IEEE Trans. Neural Network.* **2010**, *21*, 796−812.
(34) Ding, D.; Wang, Z.; Han, Q. L. Neural-network-based output-feedback control with stochastic communication protocols. *Automatica* **2019**, *106*, 221−229.
(35) Park, B. S.; Kwon, J. W.; Kim, H. Neural network-based output feedback control for reference tracking of underactuated surface vessels. *Automatica* **2017**, *77*, 353−359.
(36) Jun, Z.; Hua, Y.; Hongxia, Y.; Zhongda, T.; Runda, J. Gold recovery modeling based on interval prediction for a gold cyanidation leaching plant. *IEEE Access* **2019**, *7*, 71511−71528.
(37) Zhang, J.; Mao, Z. Z.; Jia, D. K.; He, D.-k. Real time optimization based on a serial hybrid model for gold cyanidation leaching process. *Miner. Eng.* **2015**, *70*, 250−263.
(38) Gao, B.; Cao, R.; Hou, Z.; Zhou, H. Model-free adaptive MIMO control algorithm application in polishing robot. *2017 6th Data Driven Control and Learning Systems (DDCLS)*, 2017; pp 135−140.
(39) Meng, D.; Zhang, J. Robust optimization-based iterative learning control for nonlinear systems with nonrepetitive uncertainties. *IEEE/CAA J. Autom. Sin.* **2021**, *8*, 1001−1014.
(40) Li, Y. X.; Yang, G. H. Event-based adaptive NN tracking control of nonlinear discrete-time systems. *IEEE Trans. Neural Netw. Learn. Syst.* **2018**, *29*, 4359−4369.

https://doi.org/10.1021/acsomega.2c06830
ACS Omega 2023, 8, 6559−6570